Macromolecules

ARTICLE

pubs.acs.org/Macromolecules

Modulating Two Copper(I)-Catalyzed Orthogonal "Click" Reactions for the One-Pot Synthesis of Highly Branched Polymer Architectures at 25 °C

Craig A. Bell, Zhongfan Jia, Jakov Kulis, and Michael J. Monteiro*

Australian Institute for Bioengineering and Nanotechnology, University of Queensland, Brisbane QLD 4072, Australia

Supporting Information

ABSTRACT: Controlling the rates of orthogonal "click" reactions in one-pot provides a method for designing highly branched macromolecular architectures. In this work, we constructed third generation (G3) dendrimers consisting of a wide range of chemically different polymer building blocks in one pot at 25 °C. This approach reduced the number of purification and chemical protection steps. Using the model polystyrene (PSTY) building block system, third generation dendrimers could be formed divergently, convergently or in parallel through modulating the Cu(I) activity for the copper(I)-catalyzed azide−alkyne cycloaddition (CuAAC) and nitroxide radical coupling (NRC) reactions. The parallel approach was the fastest, generating a G3 dendrimer in under 30 min, and the next fastest was the divergent pathway, followed by the very slow (24 h) convergent pathway. The resulting G3 dendrimer could be cleaved at the alkoxyamine sites back to linear polymers by heating the reaction mixture at 120 °C in the presence of an excess hydroxyl nitroxide. The synthetic utility of this method was further extended to coupling linear telechelic polymer building blocks, consisting of PSTY, P^{t}BA, PEG, and PNIPAM, to form a range of dendrimers in high yields. Preparative SEC was used to fractionate excess starting reactants and intermediate polymer species from the product dendrimer.

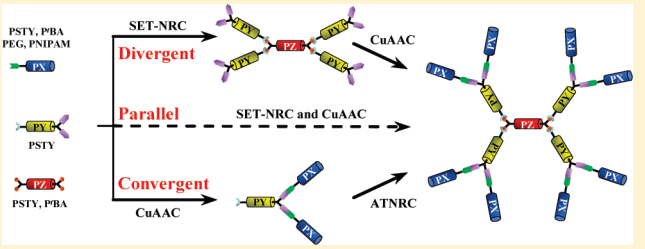

INTRODUCTION

"Living" radical polymerization (LRP) results in polymers with controlled chain length, chain length polydispersity, and chain end-group functionality. Modifying the end-groups with the appropriate chemical moieties and further reacting them through "click"-type reactions creates a wide range of polymer architectures.[1] The most common approach combines atom transfer radical polymerization (ATRP) and the copper(I)-catalyzed azide−alkyne cycloaddition (CuAAC)[2] reaction to produce functional telechelics,[3] macromonomers,[4] multiblock copolymers,[5] macrocycles,[6] stars,[7] dendrimers,[7a,8] bioconjugates,[9] and functional surfaces.[10] Examples of additional "click" reactions used to produce complex architectures from polymer building blocks include strain-promoted azide−alkyne coupling (SPAAC),[11] Diels−Alder,[12] and thiol−ene[13] reactions. These robust orthogonal chemical reactions provide a method for selectively modifying macromolecules in near-quantitative yields to create complex architectures in a controlled and predictable way.

One such structure—the dendrimer—has captured the interest of academia and industry as this is a highly branched macromolecule with precise three-dimensional molecular structure.[14] The applications of dendrimers range from drug and gene carriers to viscosity modifiers.[15] However, their synthesis via either a divergent[16] or convergent[17] approach usually requires multiple reaction steps and time-consuming purification procedures after each step. Robust and orthogonal "click" reactions as described above have been shown to increase the synthetic efficiency with fewer reaction steps.[7a,8c,13a,18] More recently, the sequential "click" coupling of asymmetric monomers produced degradable polyester dendrimers via a divergent approach, rapidly and with high efficiency.[19] This synthetic methodology required no intermediate reactions or protection and deprotection steps. In another example, the divergent approach using AB_2 and CD_2 type monomers produced a sixth generation dendrimer by combining the orthogonal CuAAC and thiol−ene coupling reactions in sequence.[13c] Precise control of the reaction order (or pathway) of orthogonal reactions will provide a powerful method for dictating not only the building block sequence but also potentially the overall macromolecular architecture as well.

Copper(I) has the ability to catalyze two "click" type reactions: azide−alkyne cycloaddition (CuAAC)[2] and the reversible nitroxide radical coupling (NRC), which includes atom transfer nitroxide radical coupling (ATNRC)[1c,20] or single electron transfer−nitroxide radical coupling (SET-NRC).[21] Our group has recently exploited the SET-NRC methodology and demonstrated its "click"-like attributes for chemical modification of polymer chain-ends with a wide variety of chemical functionality and with no side reactions.[21] The CuAAC and NRC reactions

Received: March 22, 2011
Revised: May 10, 2011
Published: May 25, 2011

Scheme 1. General Schematic for the Synthesis of G3 Polymeric Dendrimers in One Pot by NRC and CuAAC

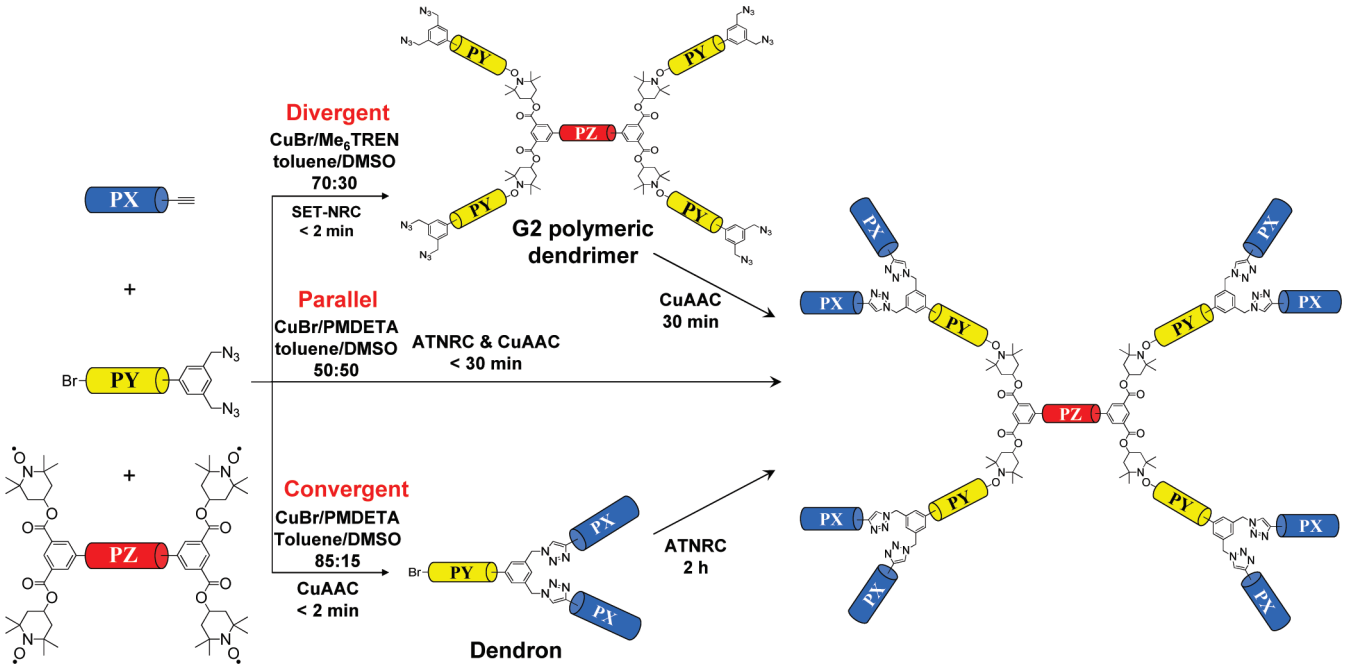

have been used separately or consecutively in the synthesis of complex molecular and macromolecular architectures. Controlling the sequence of these reactions has the potential to direct the pathway for the formation of complex macromolecules in one pot. The rate of activation of P−X (where P represents a polymer chain with a halide end-group functionality, X) to its incipient radical ($P^{\bullet}$) starting with the Cu(I)Br catalyst can be modulated by the choice of solvent/ligand combination (Scheme 1). In the presence of dimethyl sulfoxide (DMSO) and Cu(I)Br/Me_6TREN, activation proceeds via an SET mechanism.[22] Conversely, when changing to toluene and Cu(I)Br/PMDETA, activation proceeds via an atom transfer radical mechanism.[23] The rates of CuAAC reactions can also be modulated by the nature of solvent employed; a rapid CuAAC reaction occurs in toluene,[6b,c,24] but in DMSO this reaction becomes significantly slower.[24] We recently reported the directed synthesis of a second generational dendritic architecture in one pot at 25 °C by modulating the rates of these two "click" type reactions through the coupling of a trinitroxide monomer, an AB_2 type monomer incorporating two azides and one bromine, and an alkyne monomer.[21a] The synthesis of the dendrimer could proceed either in a convergent, divergent, or simultaneous pathway with very high yields by modulating the catalytic activity of Cu(I) through the choice of ligand and solvent using the conditions described above. We further demonstrated the utility of this methodology by constructing a high yielding G3 dendrimer using the CuAAC, either ATNRC or SET-NRC and thiol−ene "click" reactions. Our methodology represents a mild, versatile, and highly practical strategy for the construction of a wide range of complex macromolecular architectures.[21a]

In this work, we further exemplify the application of this methodology to create dendrimers in one pot from polymer building blocks; in particular, by coupling telechelic polymer chain building blocks to generate third generational dendritic architectures in one pot at 25 °C (Scheme 1). The synthetic pathway, either divergent, convergent, or parallel, could be directed through modulating Cu(I) activity through the choice of solvent and ligands employed. The combination of using the fastest rate of coupling conditions for both "click" type reactions and using four different polymer building blocks led to the synthesis in high yields of a wide range of G3 polymeric dendrimers in less than 30 min in one pot at 25 °C (Scheme 2).

EXPERIMENTAL SECTION

Materials. The following monomers were deinhibited before use by passing through a basic alumina column: styrene (STY: Aldrich, >99%) and *tert*-butyl acrylate (^{t}BA: Aldrich, >99%). *N*-Isopropylacrylamide (NIPAM: Aldrich, 97%) was dissolved in a minimum amount of boiling petroleum spirit, recrystallized on cooling, collected by vacuum filtration, and dried at room temperature in high vacuum before use. The following chemicals were used as received: alumina, activated basic (Aldrich, Brockmann I, standard grade, ~150 mesh, 58 Å), magnesium sulfate ($MgSO_4$: anhydrous, Scharlau, extra pure), sodium chloride (NaCl: Univar, 99.9%), sodium azide (NaN_3: Aldrich, 99.5%). The following solvents were used as received: acetone (ChemSupply, AR), chloroform ($CHCl_3$: Labscan, AR grade), dimethyl sulfoxide (DMSO: Labscan, AR grade), dichloromethane (DCM: Labscan, AR grade), diethyl ether (Merck, GR grade), ethyl acetate (EtOAc: Univar, AR grade), methanol (MeOH: anhydrous, Lichrosolv, 99.9%, HPLC grade), *N*,*N*-dimethylformamide (DMF: Labscan, AR grade), *N*,*N*-dimethylacetamide (DMAc: Aldrich, HPLC grade), petroleum spirit (BR 40−60 °C, Univar, AR grade), poly(ethylene glycol) monomethyl ether (PEG_{45}-OH: Aldrich, M_n = 2000), tetrahydrofuran (THF: Lichrosolv, HPLC grade), and toluene (TOL, Univar, AR grade). The following initiators, ligands, and metals for the various polymerizations are given below and used as received unless otherwise stated: ethyl 2-bromoisobutyrate (EBiB: Aldrich, 98%), copper(I) bromide (Cu(I)Br: Aldrich, 99.999%), copper(II) bromide ($Cu(II)Br_2$: Aldrich, 99%), *N*,*N*,*N*′,*N*′,*N*″-pentamethyldiethylenetriamine (PMDETA: Aldrich, 99%) was passed through a plug of silica (230−400 mesh) before use. Tris(2-(dimethylamino)ethyl)amine (Me_6TREN) was synthesized using the previously described method of Ciampolini et al.[25]

dx.doi.org/10.1021/ma200649b |*Macromolecules* 2011, 44, 4814–4827

Scheme 2. General Structures for the G3 Polymeric Dendrimers 14−21

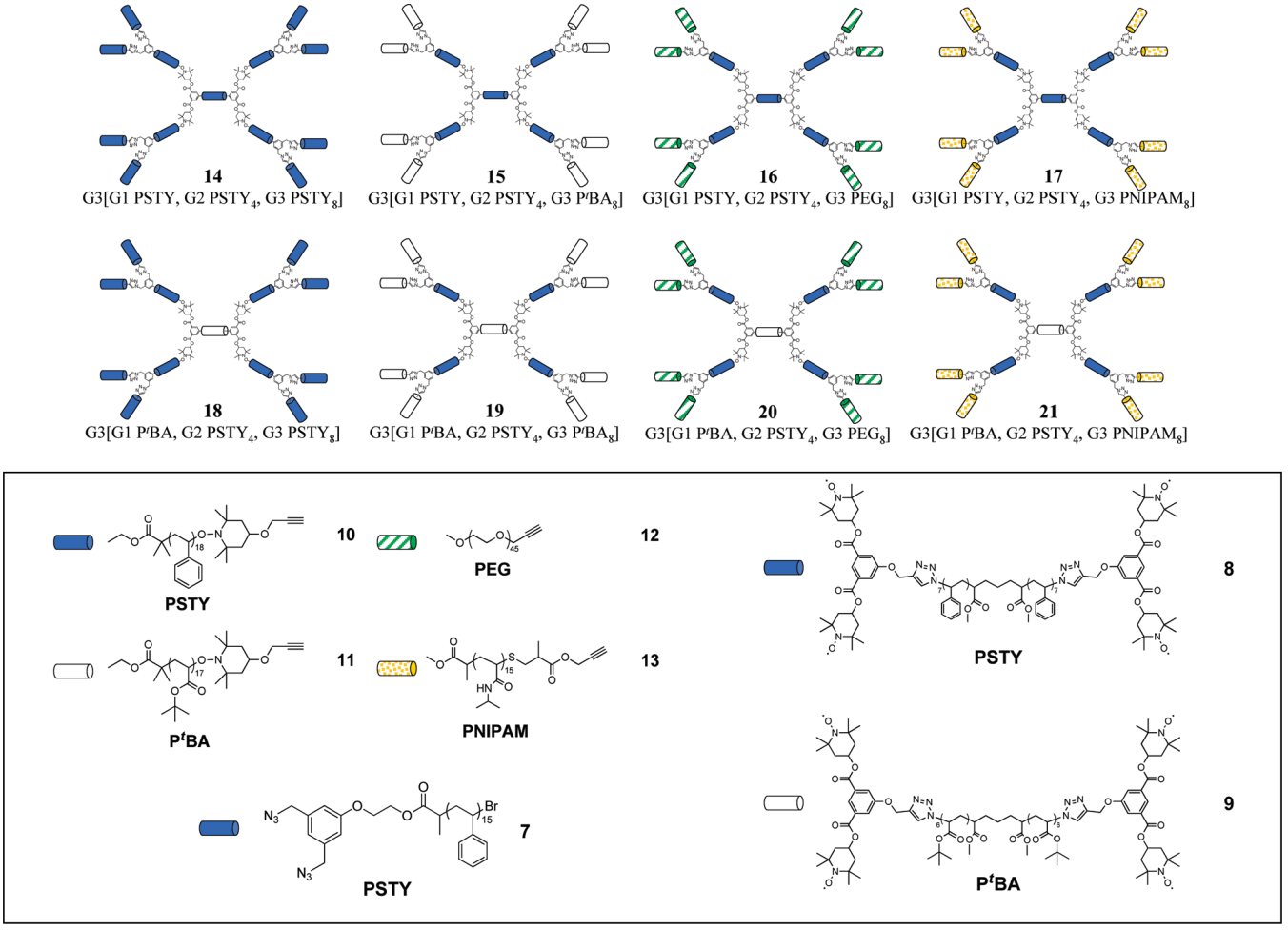

4-Hydroxy-2,2,6,6-tetramethylpiperidin-1-yloxyl (TEMPO-OH) was synthesized using the previously described method of Kulis et al.[21c,d]

Analytical Methodologies. *Size Exclusion Chromatography (SEC).* All polymer samples were dried prior to analysis in a vacuum oven for 2 days at 25 °C. The dried polymer was dissolved in tetrahydrofuran (THF) to a concentration of 1 mg/mL and then filtered through a 0.45 μm PTFE syringe filter. Analysis of the molecular weight distributions of the polymers was accomplished using a Waters 2695 separations module, fitted with a Waters 410 refractive index detector maintained at 35 °C, a Waters 996 photodiode array detector, and two Ultrastyragel linear columns (7.8 × 300 mm) arranged in series. These columns were maintained at 40 °C for all analyses and are capable of separating polymers in the molecular weight range of 500−4 million g/mol with high resolution. All samples were eluted at a flow rate of 1.0 mL/min. Calibration was performed using narrow molecular weight PSTY standards (PDI ≤ 1.1) ranging from 500 to 2 million g/mol. Data acquisition was performed using Empower software, and molecular weights were calculated relative to polystyrene standards.

Absolute Molecular Weight Determination by Triple Detection−Size Exclusion Chromatography (TD-SEC). Absolute molecular weights of polymers were determined using a Polymer Laboratories GPC50 Plus equipped with dual angle laser light scattering detector, viscometer, and differential refractive index detector. HPLC grade tetrahydrofuran and *N,N*-dimethylacetamide (DMAc, containing 0.03 wt % LiCl) was used as the eluent at a flow rate of 1.0 mL/min. Separations were achieved using two PLGel Mixed C (7.8 × 300 mm) SEC columns connected in series and held at a constant temperature of 40 °C (for THF) or two PLGel Mixed B (7.8 × 300 mm) SEC columns connected in series and held at a constant temperature of 50 °C (for DMAc + 0.03 wt % LiCl). The triple detection system was calibrated using a 2 mg/mL PSTY standard (Polymer Laboratories: M_{wt} = 110K, dn/dc = 0.185 mL/g (THF) and 0.16 mL/g (DMAc + 0.03 wt % LiCl), and IV = 0.4872 mL/g (THF) and 0.5809 (DMAc + 0.03 wt % LiCl)). Samples of known concentration were freshly prepared in THF or DMAc + 0.03 wt % LiCl and passed through a 0.45 μm PTFE syringe filter prior to injection. The absolute molecular weights and dn/dc values were determined using Polymer Laboratories Multi-Cirrus software based on the quantitative mass recovery technique. For low-MW polymers that did not have any light scattering, molecular weights were calculated from dual detection using RI and viscometer.

Preparative Size Exclusion Chromatography (Prep-SEC). Crude dendrimer structures were purified using a Varian ProStar preparative SEC system equipped with a manual injector, differential refractive index detector, and single wavelength ultraviolet−visible detector. HPLC grade tetrahydrofuran was used as eluent at flow rate of 10 mL/min. Separations were achieved using a PLgel 10 μm 10E3 Å, 300 × 25 mm preparative SEC column held at 25 °C. The dried impure polymer was dissolved in THF to give a concentration of 100 mg/mL. This solution was filtered through a 0.45 μm PTFE syringe filter prior to injection. Fractions were collected manually, and the composition of each was determined using the Polymer Laboratories GPC50 Plus equipped with triple detection as described above.

Table 1. SEC Data for All Starting Materials

product	$M_{n,SEC}$	PDI	$M_{n,DD\text{-}SEC}$[a]	PDI	dn/dc[b]	DP[c]
3	2750	1.10				25
4	2770	1.09				25
5	3180	1.09				27
6	3180	1.08				27
7	1880	1.10				14
8	2870	1.08				17
9	2810	1.08	3420	1.09	0.076	16
10	2160	1.09				18
11	1880	1.09	2470	1.09	0.055	17
12	2710	1.04	2030	1.04	0.061	45
13	2100	1.09				16

[a] Calculated from dual detection using RI and viscometer. [b] dn/dc was determined using Polymer Laboratories Multi-Cirrus software based on the quantitative mass recovery technique. [c] Degree of polymerization (DP) was determined from absolute molecular weights (where necessary) and subtraction of the incorporated functional groups.

^{1}H and ^{13}C Nuclear Magnetic Resonance (NMR). All NMR spectra were recorded on either a Bruker DRX 300 or 500 MHz spectrometer using an external lock ($CDCl_3$), and all spectra were referenced to the residual solvent peak. 1D DOSY experiments were also run to acquire ^{1}H NMR spectra of all polymers by increasing the pulse gradient from 2 to 95% of the maximum gradient strength and increasing d (p30) from 1 to 2 ms, using 256 scans. Spectra of functional molecules and polymers containing nitroxide radicals were measured in the presence of phenylhydrazine under an inert atmosphere to actively reduce the nitroxides to their incipient hydroxylamines.

Attenuated Total Reflectance—Fourier Transform Spectroscopy (ATR-FTIR). ATR-FTIR spectra were obtained using a horizontal, single bounce, diamond ATR accessory on a Nicolet Nexus 870 FT-IR. Spectra were recorded between 4000 and 500 cm^{-1} for 32 scans at 4 cm^{-1} resolution with an OPD velocity of 0.6289 cm/s. Solids were pressed directly onto the diamond internal reflection element of the ATR without further sample preparation.

Matrix-Assisted Laser Desorption Ionization—Time of Flight (MALDI-ToF) Mass Spectrometry. MALDI-ToF MS spectra were obtained using a Bruker MALDI-ToF autoflex III smartbeam equipped with a nitrogen laser (337 nm, 200 Hz maximum firing rate) with a mass range of 600−400 000 Da. All spectra of low molecular weight polymers were recorded in a reflectron mode (1500−4500 Da), and high molecular weight polymers were recorded in a linear mode (4−40 kDa). *trans*-2-[3-(4-*tert*-Butylphenyl)-2-methyl-propenylidene]malononitrile (DCTB; 20 mg/mL in THF) and 2-(4-hydroxyphenylazo)benzoic acid (HABA; 20 mg/mL in THF) were used as the matrices and Ag(CF_3COO) (2 mg/mL in THF), Na(CF_3COO), and K(CF_3COO) (2 mg/mL in THF) as the salt cation sources. Samples were prepared by mixing the matrix (20 μL), salt (2 μL) and polymer (20 μL, 1 mg/mL in THF) solutions, spotting 1 μL onto the target plate, and drying prior to analysis.

Low-Resolution Electrospray Ionization—Mass Spectrometry (LR-ESI-MS). All mass spectra were recorded on a Bruker Esquire HCT (High Capacity 3D ion trap) instrument with a Bruker ESI source and positive ion model with a mass range up to an m/z ratio of 2000 Da. Samples were prepared by dissolving the polymer/molecule in DCM then adding MeOH such that the final concentration was 1 mg/mL in a 2:3 v/v DCM/MeOH solution. To this, a 10 mg/mL solution of NaI in MeOH (10 μL) was added, and the final solution was injected via a gastight syringe.

Polymer Synthesis. *Synthesis of ATRP Polymers.* A typical ATRP polymerization procedure was as follows: freshly purified styrene (36.08 g, 0.173 mol), PMDETA (0.75 mL, 3.59 × 10^{-3} mol), EBiB (1.29 mL, 8.76 × 10^{-3} mol), and Cu(I)Br_2/PMDETA (0.35 g, 8.70 × 10^{-4} mol) were added to a 50 mL Schlenk flask equipped with a magnetic stirrer then purged with argon for 20 min. Cu(I)Br (0.62 g, 4.34 × 10^{-3} mol) was carefully added under positive argon flow, and the reaction mixture was purged with argon for 5 more min. The flask was placed in a temperature-controlled oil bath at 80 °C for 8 h. The reaction was halted by quenching in ice followed by exposure to air. The polymerization mixture was diluted with DCM, and the copper salts were removed by passage through an activated basic alumina column. The solution was concentrated by rotary evaporation, and the polymer was recovered by precipitation into methanol and then filtered and dried for 48 h under high vacuum at 25 °C. The polymer was characterized by SEC (M_n = 2750, PDI = 1.10).

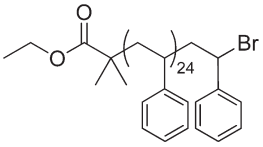

$PSTY_{25}$-Br (**3**)

Azidation of ATRP Polymers. A typical azidation procedure was as follows: NaN_3 (1.33 g, 2.04 × 10^{-2} mol) was added to a stirred solution of **3** (5.00 g, 1.82 × 10^{-3} mol) in DMF (25 mL). The reaction mixture was then stirred for 24 h at room temperature. The polymer was precipitated into methanol (twice: once from DMF, once from DCM), recovered by vacuum filtration, and washed exhaustively with water and methanol. The polymer was dried under high vacuum for 48 h at 25 °C and then characterized by SEC (M_n = 2770, PDI = 1.09).

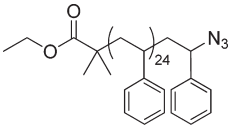

$(PSTY)_{25}$-N_3 (**4**)

Typical NRC Functionalization of a Bromine Functional Polymer. A typical NRC procedure was as follows: **3** (2.50 g, 9.09 × 10^{-4} mol) was added to a stirred solution of TEMPO−≡ (0.26 g, 1.22 × 10^{-3} mol) and Me_6TREN (0.29 g, 1.25 × 10^{-3} mol) in 50% v/v toluene/DMSO (25 mL). The reaction mixture was then purged with argon for 20 min. Cu(I)Br (0.176 g, 1.22 × 10^{-3} mol) was then added to the solution under a positive flow of argon, and the reaction mixture was sealed and stirred for 1 h at 25 °C in a temperature-controlled oil bath. The polymer was diluted with DCM, and the copper salts were removed by passage through an activated basic alumina column. The solution was concentrated by rotary evaporation, and the polymer was recovered by precipitation (twice: once from toluene/DMSO, once from DCM) into methanol, collected by vacuum filtration, and washed exhaustively with methanol. The polymer was dried under high vacuum for 48 h at 25 °C and then characterized by SEC (M_n = 3180, PDI = 1.08).

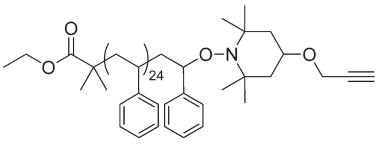

$(PSTY)_{25}$-≡ (**5**)

Typical CuAAC Functionalization of an Azide Functional Polymer. A typical CuAAC procedure was as follows: **4** (2.50 g, 9.01 × 10^{-4} mol)

dx.doi.org/10.1021/ma200649b |*Macromolecules* 2011, 44, 4814–4827

Scheme 3. General Schematic for the Synthesis of Br, Nitroxide, Azide, and Alkyne Functional PSTY and the Determination of Coupling Rates by NRC and CuAAC in Various Toluene/DMSO Solvent Ratios

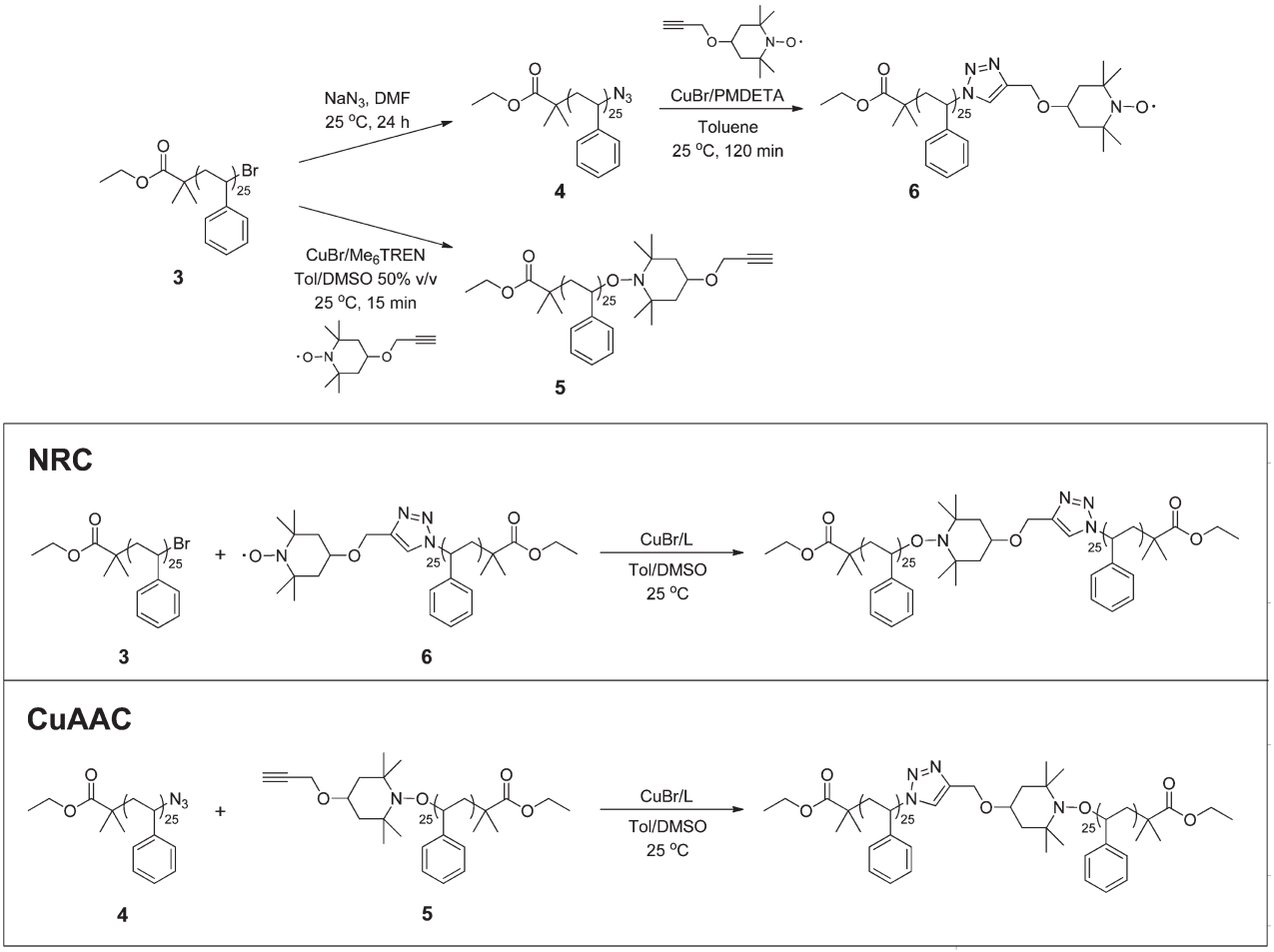

was added to a stirred solution of TEMPO—≡ (0.26 g, 1.25×10^{-3} mol) and Me_6TREN (0.12 g, 5.00×10^{-4} mol) in toluene (25 mL). The reaction mixture was then purged with argon for 20 min. Cu(I)Br (0.072 g, 5.00×10^{-4} mol) was then added to the solution under a positive flow of argon, sealed, and stirred for 2 h at 25 °C in a temperature-controlled oil bath. The polymer was diluted with DCM, and the copper salts were removed by passage through an activated basic alumina column. The solution was concentrated by rotary evaporation, and the polymer was recovered by precipitation (twice: once from toluene, once from DCM) into methanol, collected by vacuum filtration, and washed exhaustively with methanol. The polymer was dried under high vacuum for 48 h at 25 °C and then characterized by SEC (M_n = 3180, PDI = 1.09).

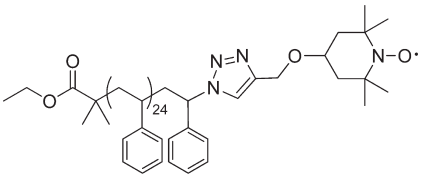

$(PSTY)_{25}$-NO· (**6**)

*Synthesis of PEG_{45}—≡ (**12**).* Sodium hydride (0.51 g, 1.28×10^{-2} mol) was added to dry THF (25 mL) under argon and cooled to 0 °C. To this suspension, PEG_{45}-OH (5.00 g, 2.50×10^{-3} mol) was added portionwise and stirred until dissolved before propargyl bromide (1.39 mL, 1.25×10^{-2} mol) was added directly. The solution was stirred at 0 °C for 30 min and then at room temperature for 24 h, after which saturated NH_4Cl solution (10 mL) was slowly added to quench the reaction. The solution was then extracted with DCM (50 mL), and the organic phase was then washed with brine (3 × 50 mL). The organic phase was collected, dried with anhydrous magnesium sulfate, filtered, and evaporated to dryness. The light brown solid was redissolved in a minimum volume of DCM and precipitated (twice) into diethyl ether. The solid was then collected by vacuum filtration, washed with diethyl ether, collected, and dried in vacuo at 25 °C for 48 h. The resultant white polymer was characterized by SEC (M_n = 2710, PDI = 1.04) and dual detection SEC (M_n = 2030, PDI = 1.04, dn/dc = 0.061).

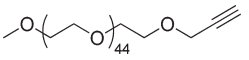

*Synthesis of $PNIPAM_{15}$—≡ (**13**).* $PNIPAM_{15}$—SC(═S)SC_4H_9 was synthesized according to the procedure of Urbani et al.[26] and was characterized by SEC using PSTY standards (M_n = 1900, PDI = 1.09).

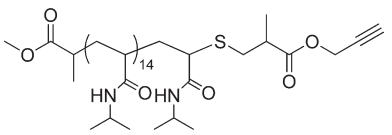

$PNIPAM_{15}$—SC(═S)SC_4H_9 (1.01 g, 5.32×10^{-4} mol), propargyl methacrylate (0.65 g, 5.39×10^{-3} mol), and TCEP·HCl (2.47×10^{-2} g,

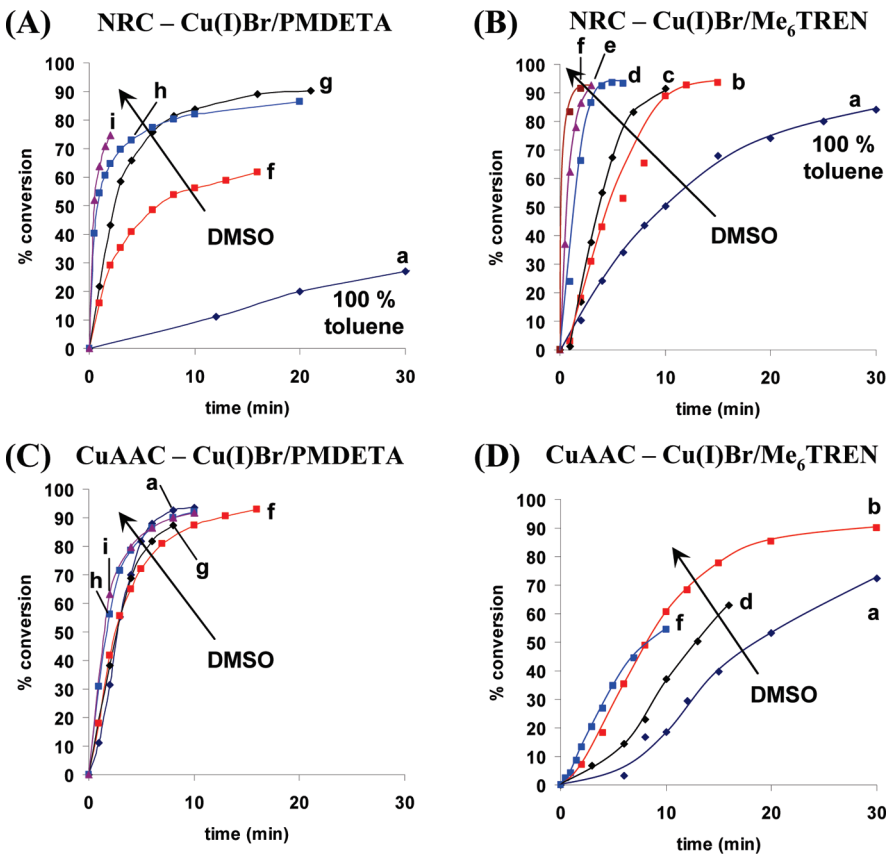

Figure 1. Kinetic data for 2-arm star formation with varying DMSO to toluene ratios. (A) NRC of **3** and **6** using Cu(I)Br/PMDETA, (B) CuAAC of **4** and **5** using Cu(I)Br/PMDETA, (C) NRC of **3** and **6** using Cu(I)Br/Me_6TREN, (D) CuAAC of **4** and **5** using Cu(I)Br/Me_6TREN. Varying % v/v toluene:DMSO: curves (a) 100:0, (b) 90:10, (c) 85:15, (d) 80:20, (e) 75:25, (f) 70:30, (g) 50:50, (h) 40:60, and (i) 30:70.

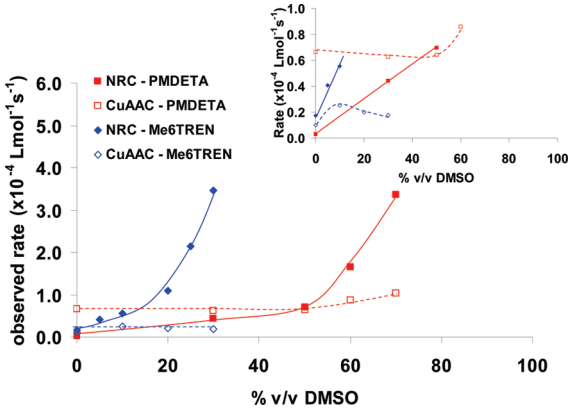

Figure 2. Rate of formation of poly(styrene) diblock from CuAAC and NRC in different solvent ratios of toluene and DMSO using either Cu(I)Br/PMDETA or Cu(I)Br/Me_6TREN.

8.62×10^{-5} mol) were dissolved in DMF (5 mL) and degassed by argon purge for 30 min. A separate vial containing hexylamine was also purged with argon for 30 min. After this time, 348 μL (0.27 g, 2.63×10^{-3} mol) was added to the first solution via a gastight syringe, and the reaction was stirred at room temperature for 24 h. The solution turned from light yellow to clear with the cleavage of the RAFT end group. Afterward, the solution was precipitated (twice: once from DMF, once from THF) into diethyl ether/PET spirit (50% v/v) and filtered, washing with PET spirit. The precipitate was collected and dried under vacuum at RT for 48 h and was characterized by SEC using PSTY standards (M_n = 2100, PDI = 1.09).

SEC characterization of all starting reagents used in the kinetics and synthesis of the G3 polymeric dendrimers can be found in Table 1.

Kinetics. *CuAAC "Click" Kinetics.* An example reaction was as follows: **4** (0.055 g, 2.00×10^{-5} mol), **5** (0.064 g, 2.00×10^{-5} mol), PMDETA (3.46×10^{-3} g, 2.00×10^{-5} mol), and toluene (1 mL) were all added to a 10 mL Schlenk flask equipped with a magnetic stirrer. The reaction mixture was then degassed by three successive freeze−pump−thaw cycles, after which the reaction was placed in a 25 °C water bath under argon to thermally equilibrate and Cu(I)Br (2.87×10^{-3} g, 2.00×10^{-5} mol) was carefully added under a positive flow of argon. The mixture was then sealed under argon and stirred. Samples were taken periodically and analyzed by SEC.

NRC Kinetics. An example reaction was as follows: **3** (0.055 g, 2.00×10^{-5} mol), **6** (0.064 g, 2.00×10^{-5} mol), Me_6TREN (4.61×10^{-3} g, 2.00×10^{-5} mol), and toluene (1 mL) were all added to a 10 mL Schlenk flask equipped with a magnetic stirrer. The reaction mixture was then degassed by three successive freeze−pump−thaw cycles, after which the reaction was placed in a 25 °C water bath under argon to thermally equilibrate and Cu(I)Br (2.87×10^{-3} g, 2.00×10^{-5} mol) was carefully added under a positive flow of argon. The mixture was then sealed under argon and stirred. Samples were taken periodically and analyzed by SEC.

G3 Polymeric Dendrimer Kinetics. An example reaction was as follows: **8** (1.00×10^{-2} g, 3.5×10^{-3} M, 1 equiv), **7** (2.73×10^{-2} g, 1.4×10^{-2} M, 4.1 equiv), **10** (6.34×10^{-2} g, 2.9×10^{-2} M, 8.4 equiv), Me_6TREN (6.43×10^{-3} g, 2.8×10^{-2} M, 8 equiv), and toluene/DMSO (70:30 v/v, 1 mL) were all added to a 10 mL Schlenk flask equipped with

dx.doi.org/10.1021/ma200649b |*Macromolecules* 2011, 44, 4814–4827

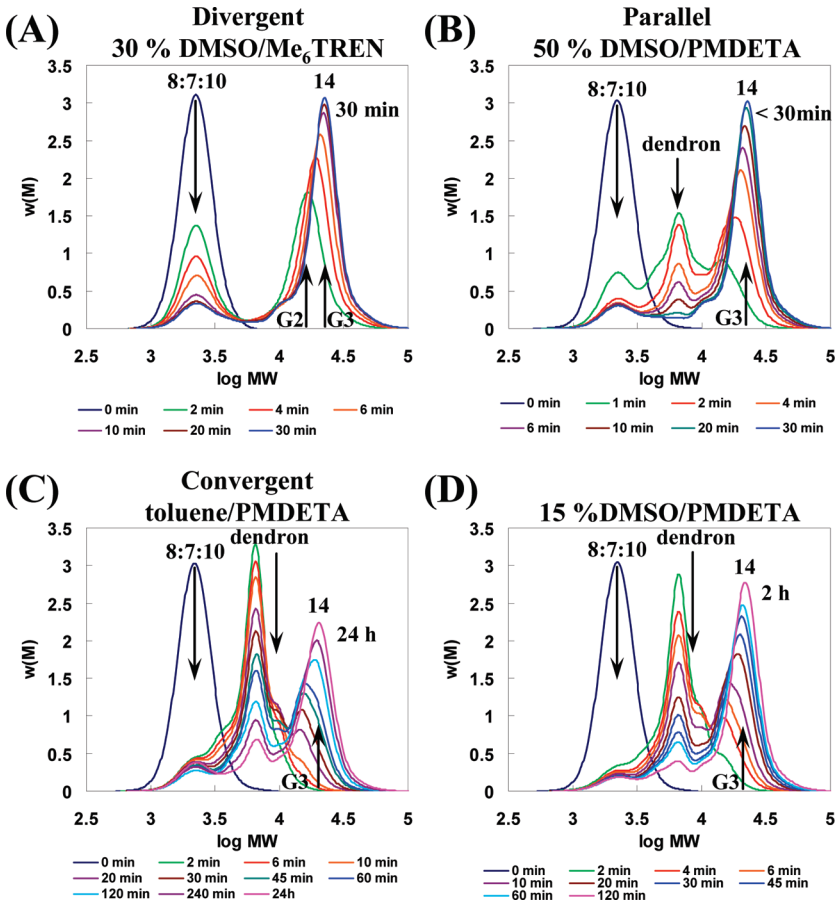

Figure 3. Molecular weight distributions (based on the weight distribution, $w(M)$) for the synthesis of third generation PSTY dendrimer using a tetrafunctional nitroxide PSTY core: (A) divergent synthesis in 30% v/v DMSO in toluene using Me_6TREN, (B) parallel synthesis in 50% v/v DMSO in toluene using PMDETA, (C) convergent synthesis in 100% toluene using PMDETA, and (D) faster convergent synthesis in 15% v/v DMSO in toluene using PMDETA. [**8**]:[**7**]:[**10**]:[Cu(I)Br]:[PMDETA/Me_6TREN] = 1:4.1:8.4:8:8. [**8**] = 3.5×10^{-3} M.

a magnetic stirrer. The reaction mixture was then degassed by sparging with argon for 30 min, after which the reaction was placed in a 25 °C water bath under argon to thermally equilibrate and Cu(I)Br (4.00×10^{-3} g, 2.8×10^{-2} M, 8 equiv) was carefully added under a positive flow of argon. The mixture was then sealed under argon and stirred. Samples were taken periodically and analyzed by SEC.

G3 Polymeric Dendrimer Synthesis. An example reaction was as follows: **8** (1.50×10^{-2} g, 3.5×10^{-3} M, 1 equiv), **7** (4.04×10^{-2} g, 1.4×10^{-2} M, 4.1 equiv), **11** (1.09×10^{-1} g, 2.9×10^{-2} M, 8.4 equiv), PMDETA (7.25×10^{-3} g, 2.8×10^{-2} M, 8 equiv), and toluene/DMSO (50:50 v/v, 1.5 mL) were all added to a 10 mL Schlenk flask equipped with a magnetic stirrer. The reaction mixture was then degassed by sparging with argon for 30 min, after which the reaction was placed in a 25 °C water bath under argon to thermally equilibrate and Cu(I)Br (6.00×10^{-3} g, 2.8×10^{-2} M, 8 equiv) was carefully added under a positive flow of argon. The mixture was then sealed under argon and stirred. Samples were taken periodically and analyzed by SEC. The resultant polymeric dendrimer G3[G1 PSTY, G2 $PSTY_4$, G3 P^tBA_8] (**15**) was purified by preparative SEC.

Decoupling of PSTY G3 Polymeric Dendrimer. G3[G1 PSTY, G2 $PSTY_4$, G3 $PSTY_8$] (**14**) (M_n = 25 830, 1.51×10^{-2} g, 3.90×10^{-4} M), TEMPO-OH (2.66×10^{-2} g, 0.1 M, 20 equiv per alkoxyamine), and toluene (1.5 mL) were all added to a 10 mL Schlenk flask equipped with a Teflon stopper and a magnetic stirrer. The reaction mixture was then degassed by sparging with argon for 30 min, after which the reaction was sealed and placed in a 120 °C oil bath and stirred for 5.5 h. After this time, the reaction was cooled to room temperature and sampled for MALDI-ToF and SEC analysis.

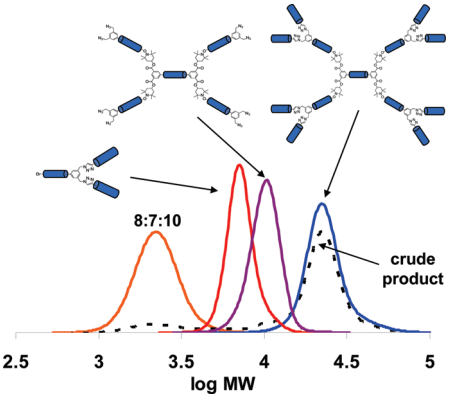

Figure 4. Molecular weight distributions (based on the weight distribution, $w(M)$) of the starting reactant mixture, the wedge dendron, PSTY G2 polymeric dendrimer, and PSTY G3 polymeric dendrimer (**14**) before and after preparative SEC purification.

RESULTS AND DISCUSSION

"Click" Coupling Kinetics of PSTY Model System. Directing the pathway of CuAAC and NRC reactions requires knowledge

dx.doi.org/10.1021/ma200649b |*Macromolecules* 2011, 44, 4814–4827

Table 2. Size Exclusion Chromatographic (SEC) Data for the Synthesis of Structures 14−21

reactants[a]	product	% coupling efficiency[b]	$M_{n,SEC}$	PDI	$M_{n,TD\text{-}SEC}$	$M_{p,TD\text{-}SEC}$	$M_{n,theory}$[c]	$M_{p,theory}$[d]	PDI	dn/dc (dn/dc_{theory}[e])
7, 8, 10	**14**	86	21 190	1.12	25 830	27 180	27 680	27 100	1.10	0.168 (0.185)
7, 8, 11	**15**	98	22 300	1.11	29 530	30 880	30 170	29 500	1.09	0.098 (0.100)
7, 8, 12	**16**	88	26 840	1.15	24 820	27 340	26 670	26 100	1.08	0.108 (0.110)
7, 8, 13	**17**	93	21 580	1.16	26470[f]	27 240	26 400	26 500	1.14	0.098 (0.102)
7, 9, 10	**18**	80	20 990	1.12	27 820	28 440	28 230	27 500	1.11	0.127 (0.172)
7, 9, 11	**19**	87	20 290	1.09	29 300	34 209	30 720	29 900	1.11	0.104 (0.103)
7, 9, 12	**20**	76	24 110	1.12	31 780	28 030	27 220	26 500	1.10	0.111 (0.098)
7, 9, 13	**21**	81	20 640	1.13	28490[f]	28 770	27 750	27 100	1.03	0.088 (0.089)

[a] Stoichiometries for all reactions were as follows: core, 1 equiv; first generational layer, 4.1 equiv; and second generational layer, 8.4 equiv. [b] Determined from the % area of the product peak to % total area in the SEC trace. The efficiency (based on the different stoichiometric ratios of the reactants and the dead polymer content of each species) to theoretical efficiency gives a value for the % efficiency. [c] $M_{n,theory}$ was calculated based on the MW of the starting materials analyzed by TD-SEC. [d] Determined from log-normal distributions (see Supporting Information for distribution formulas). [e] dn/dc_{theory} was calculated based on the weight fraction of incorporated polymers and their individual dn/dc's according to the equation $dn/dc_{final} = w_A(dn/dc_A) + w_B(dn/dc_B) + w_C(dn/dc_C)$. [f] Analyzed in DMAc + 0.03 wt % LiCl using a $dn/dc = 0.065$ for PNIPAM due to its incorporation into the final dendrimer.

of the relative rates of coupling in different solvent conditions with different ligands. We used polystyrene (PSTY) building blocks as the model system (see Scheme 3). In the first set of coupling reactions, polymers **3** and **6** were coupled via the NRC approach using PMDETA (Figure 1A) or Me_6TREN (Figure 1B) as ligand and varying the solvent ratio of toluene to DMSO. We used various toluene and DMSO solvent mixtures in which PSTY was soluble, since PSTY was not soluble in 100% DMSO. In the presence of PMDETA, the rate of NRC reaction rapidly increased by changing from 100% toluene (Figure 1A, curve a, 30% conversion after 30 min) to the addition of 30% DMSO (i.e., 30% DMSO and 70% toluene, Figure 1A, curve f). Increasing the DMSO content to 70% (Figure 1A, curve i) showed a significant increase in the rate, reaching 80% conversion in less than 2 min. Changing the ligand to Me_6TREN showed a similar trend with increasing DMSO to that with PMDETA, but in this case the rate was significantly faster even in 100% toluene (Figure 1B, curve a). The addition of only 10% DMSO (Figure 1B, curve b) resulted in a fast NRC reaction rate, reaching high conversions after only 10 min. This rate further increased with the addition of 30% DMSO as cosolvent (Figure 1B, curve f). These trends were in agreement with previous results for NRC.[21a,d] In the SET-NRC process, the combination of DMSO solvent and Me_6TREN ligand has been shown to facilitate disproportionation of Cu^I to Cu^0 and Cu^{II},[27] in which the high activating Cu^0 converts the halide to its incipient radical.[22a] Experiments using nitroxides to trap these incipient radicals showed the extremely rapid rate of radical formation.[21c,d]

In the second set of experiments, the coupling of polymers **4** and **5** (see Scheme 3) via the CuAAC reaction using PMDETA (Figure 1C) or Me_6TREN (Figure 1D) as ligand and varying the solvent ratio of toluene to DMSO showed that DMSO had a much smaller effect on the CuAAC reaction compared to the NRC reaction. In the presence of the ligand, PMDETA (Figure 1C), DMSO had little or no effect on the CuAAC rate. When Me_6TREN (Figure 1D) was used as the ligand, the rates of CuAAC were much slower than in the presence of PMDETA, with no discernible influence on the ratio of DMSO used. This result is consistent with previous literature observations.[24] We believe that the rapid rate of CuAAC regardless of solvent in the presence of PMDETA is due to the ability of the Cu(I)Br/PMDETA to be highly soluble in all toluene/DMSO solvent ratios. Cu(I)Br/PMDETA forms a neutral, distorted square-planar complex when coordinated with Br^-,[28] but can also form other charged, distorted tetrahedral complexes with solvents and monomer species.[29] The slower rate in the presence of Me_6TREN suggests that DMSO can interfere in the Cu^I catalytic cycle of the CuAAC reaction. It should be noted that DMSO will not interfere with the SET-NRC reaction with Me_6TREN since Cu^0 and not Cu^I is the activating catalyst.

To exemplify the synthetic direction of dendrimer formation (divergent, convergent, or simultaneous formation; see Scheme 1) using these two "click" type reactions, we need to choose the appropriate ligand and solvent combinations. The observed initial rates of CuAAC and NRC reactions presented in Figure 1 are summarized in Figure 2. The NRC reaction was significantly slower than the CuAAC reaction in PMDETA and 100% toluene (inset in Figure 2), resulting in conditions for a convergent pathway (see Scheme 1). To increase the rate of this reaction pathway without compromising the convergent process, up to 20% DMSO can be added. To direct the pathway via a divergent approach, NRC must be much faster than the CuAAC reaction. The kinetic profiles in Figure 2 show that Me_6TREN significantly enhanced the rate of SET-NRC over the CuAAC reaction above 20% DMSO. For both reactions to occur simultaneously (or in parallel), the kinetic profiles indicated that PMDETA should be used as the ligand in combination with solvent conditions between 30 and 50% DMSO.

Directed Synthesis of G3[G1PSTY$_1$, G2PSTY$_4$, G3PSTY$_8$] via Divergent, Convergent, or Simultaneous Pathway. Generally, there are two different methods for the synthesis of dendrimers: divergently through the addition of small units "growing out" from a starting core structure or convergently through addition of smaller units to form dendrons that couple to then form a dendrimer.[30] Primarily, either synthesis utilizes an AB_2 type monomer to incorporate branching points for the eventual assembly into dendrimers. In this work, we used three types of polymers: a tetranitroxide functional core polymer, a telechelic AB_2 type polymer consisting of two azides and an activated bromine, and a linear, alkyne functional polymer (Scheme 1). Based on the kinetic profiles from the previous section, the use of four different synthetic conditions produced a G3 dendrimer in one pot at 25 °C. These conditions were as follows: the combination of 30% DMSO with Cu(I)Br/Me_6TREN resulted in a divergent pathway, the combination of 50%

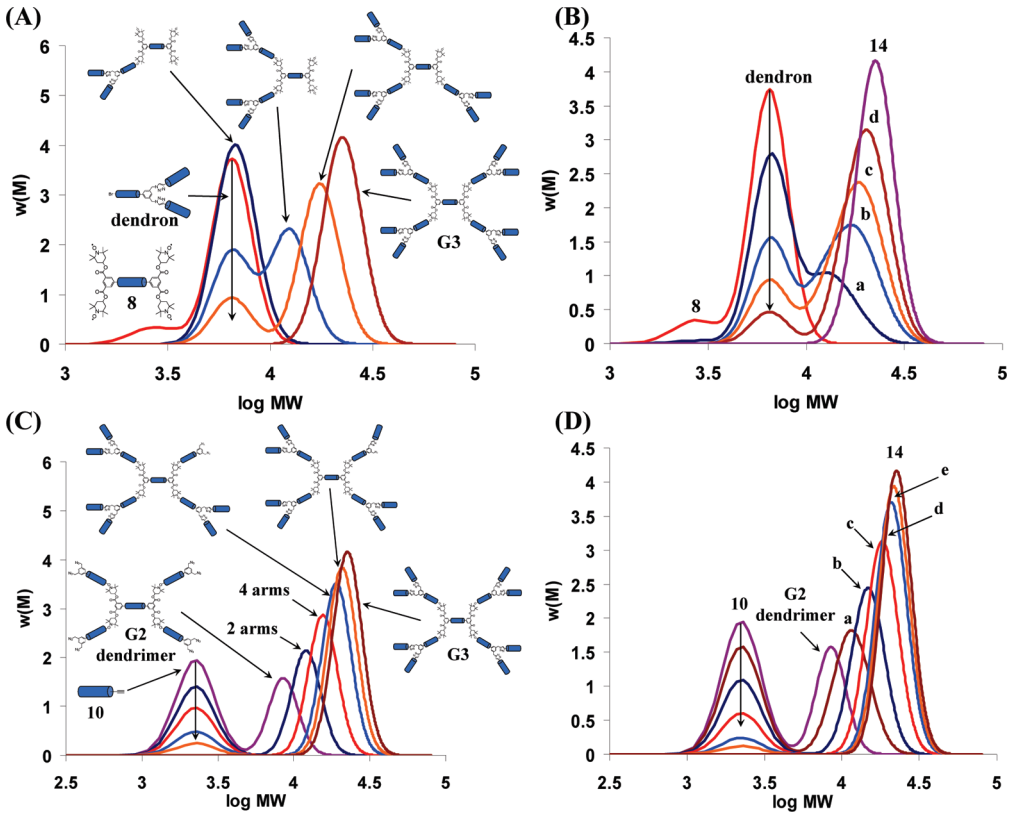

Figure 5. Simulations of the molecular weight distributions (based on $w(M)$) determined from the log-normal distribution (see Supporting Information). (A) Simulated MWDs formed convergently with 0, 1, 2, 3, and 4 dendrons attaching onto **8**. (B) Simulated MWDs formed convergently with 0, 1, 2, 3, and 4 dendrons attaching onto **8**. (a) **8**:**8** + 1 dendron:**8** + 2 dendrons:**8** + 3 dendrons = 1:3:3:1, (b) **8** + 1 dendron:**8** + 2 dendrons:**8** + 3 dendrons:**14** = 1:3:3:1, (c) **8** + 2 dendrons:**8** + 3 dendrons:**14** = 1:2:1, (d) **8** + 3 dendrons:**14** = 1:1. (C) Simulated MWDs formed divergently with 0, 2, 4, 6, 7 and 8 second generational arms (**10**) attaching onto a G2 dendrimer. (D) Simulated MWDs formed divergently with 2, 3, 4, 5, 6, 7 and 8 second generational arms (**10**) attaching onto a G2 dendrimer in various stochastic ratios. (a) **G2** + 2 arms:**G2** + 3 arms:**G2** + 4 arms:**G2** + 5 arms = 1:3:3:1, (b) **G2** + 3 arms:**G2** + 4 arms:**G2** + 5 arms:**G2** + 6 arms = 1:3:3:1, (c) **G2** + 4 arm:**G2** + 5 arm:**G2** + 6 arms:**G2** + 7 arms = 1:3:3:1, (d) **G2** + 6 arms:**G2** + 7 arms:**14** = 1:2:1, (e) **G2** + 7 arms:**14** = 1:1.

DMSO with Cu(I)Br/PMDETA resulted in a parallel pathway, the combination of 100% toluene with Cu(I)Br/PMDETA resulted in a convergent pathway, and the combination of 15% DMSO with Cu(I)Br/PMDETA resulted in a faster convergent pathway. The reactions under these four sets of ligand and solvent conditions analyzed by SEC in Figure 3 demonstrated that modulating the CuAAC and NRC reactions of PSTY chains directed the pathway to form a G3 dendrimer. Analysis of these reactions using SEC provided the rates of formation of intermediates and the resulting product, allowing us to identify the reaction pathway. In Figure 4, the SEC chromatograms for all the intermediates, including the dendron and G2 dendrimer intermediates, were well resolved from both starting polymer building blocks (**7**, **8**, and **10**) and the final G3 dendrimer product. This aided in the identification of intermediate structures by SEC in Figure 3.

The use of 30% DMSO and Cu(I)Br/Me_6TREN resulted in the rapid SET-NRC coupling between **7** and **8** to form a G2 dendrimer (G2[G1PSTY$_1$, G2PSTY$_4$]) after only 2 min (Figure 3A, green curve). The SEC chromatograms show the stochastic molecular weight distribution (MWD) of intermediate species from the CuAAC of **10** to the G2 dendrimer, until no observed change after 30 min in the final chromatogram representing that of the G3 dendrimer (G3[G1PSTY$_1$, G2PSTY$_4$, G3PSTY$_8$]). The number-average molecular weight (M_n) and peak maximum molecular weight (M_p) of the G3 dendrimer found from this experiment were close to theoretically calculated values (Table 2) with an overall coupling efficiency of 86%. This reaction demonstrates the rapid SET-NRC reaction followed by the slower CuAAC reaction to form the dendrimer via a divergent pathway (Scheme 1). Changing the solvent condition to 50% DMSO and ligand to PMDETA resulted in the rapid loss of reactants, the formation of a dendron (see Figure 4), and formation of G2 dendrimer after only 1 min (Figure 3B). After 1 min, the SEC chromatograms showed the slow growth toward the G3 dendrimer. The chromatogram after 30 min gave near identical MWDs with the final G3 dendrimer found from the previous reaction together with near identical M_n and M_p values. The assembly of the G3 dendrimer can only occur via a simultaneous or parallel pathway. Using PMDETA and 100% toluene resulted in the disappearance of most of the reactants after only 2 min to form the dendron (Figure 3C, green curve)—following the convergent pathway. There was no evidence for the formation of the G2 dendrimer or any higher molecular weight species. After 2 min, the reaction proceeded slowly over 24 h to produce the G3 dendrimer with some remaining dendron. This suggests that due to the slow NRC reaction, steric hindrance, low concentration of nitroxides and bromide functional groups, and a buildup of the deactivating Cu(II)Br_2 species, we would require substantially more time to obtain high overall coupling efficiency

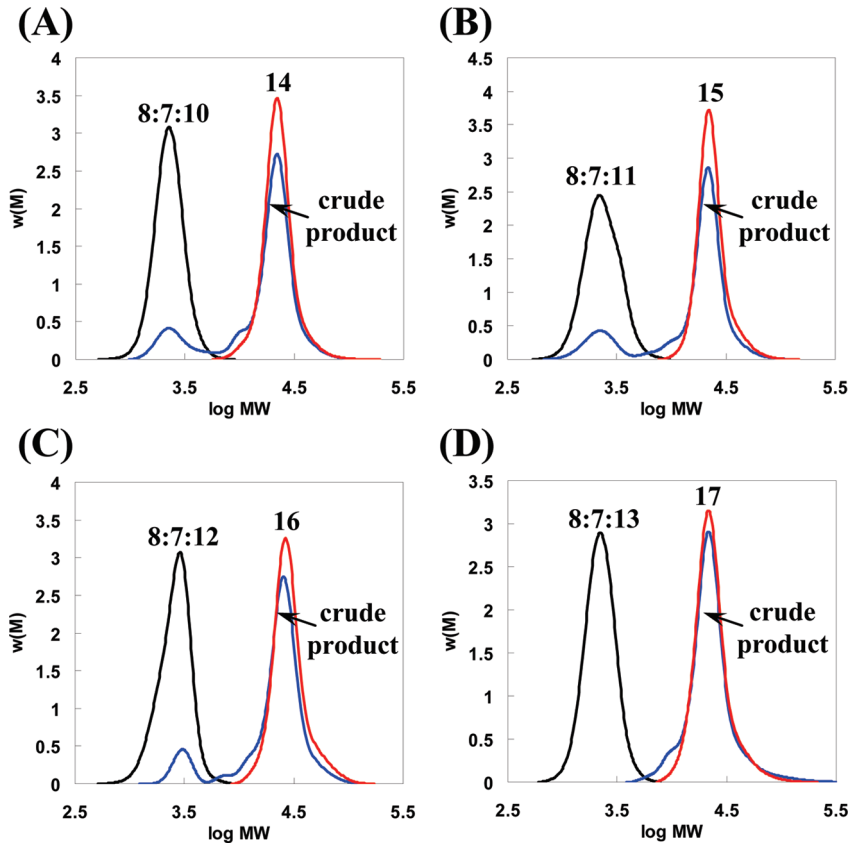

Figure 6. Size exclusion chromatography (SEC) traces for the synthesis of the G3 dendrimer via parallel technique with the PSTY core (**8**) at 25 °C using DMSO as solvent and PMDETA as ligand. (A) PSTY−$PSTY_4$−$PSTY_8$ (**14**); **8**:7:**10**:PMDETA:Cu(I)Br = 1:4.1:8.4:8:8, (B) PSTY−$PSTY_4$−P^tBA_8 (**15**); **8**:7:**11**:PMDETA:Cu(I)Br = 1:4.1:8.4:8:8, (C) PSTY−$PSTY_4$−PEG_8 (**16**); **8**:7:**12**:PMDETA:Cu(I)Br = 1:4.1:8.4:8:8, (D) PSTY−$PSTY_4$−$PNIPAM_8$ (**17**); **8**:7:**13**:PMDETA:Cu(I)Br = 1:4.1:8.4:8:8.

and high purity dendrimer. Based on our kinetic data in Figure 2, the addition of 15% DMSO should accelerate the convergent pathway (Figure 3D). Indeed, the reaction was significantly faster, with the dendron and some higher molecular weight species forming after only 2 min. The G3 dendrimer formed with high coupling efficiency and only a small amount of remaining dendron after 2 h. The results here demonstrate that the parallel pathway was the most efficient route to obtain high coupling efficiency and yields for G3 dendrimer synthesis.

The SEC traces from Figure 3C,D show evidence of a convergent pathway, specifically the formation of the dendron after 2 min. However, the formation toward the G3 dendrimer after this time was quite difficult to elucidate. Simulations of the SEC traces using log-normal distributions[31] provided the assembly mechanism for the convergent approach. Simulated SEC distributions based on a weight distribution in Figure 5A show how the MWD changes through the sequential addition of dendrons onto the core (polymer **8**). The simulated MWDs, normalized to weight, accounted for unreacted compounds. The peak maximum of the one dendron addition to **8** shifted marginally compared to the dendron itself. The M_p then shifted substantially when coupling 2, 3, and 4 dendrons to **8**. These MWDs were not similar to those observed in Figure 3C,D. There seemed to be a much more subtle change in M_p especially for the high molecular weight species. Simulations were then carried out using a stochastic approach as shown in Figure 5B, in which we used the stochastic distribution of species based on Pascall's triangle. For example, if the three dendrons attached to **8** was the main species, then the system would comprise of two dendrons attached to **8** and product **14** (using the molar ratios as follows: **8** + 2 dendrons:**8** + 3 dendrons:**14** = 1:2:1). It can now be seen that there was a shift in the peak maximum to the G3 dendrimer similar to that observed in Figure 3C,D. In the case of the divergent pathway (Figure 3A), we also simulated the MWDs (Figure 5C,D). Figure 5C shows the simulations for coupling from one to eight **10** polymer blocks onto a G2 dendrimer. The peak maximum increased with each successive attachment of **10**. These MWD profiles did not resemble the subtle changes observed from the experimental SEC traces in Figure 3A. Again, using stochastic distributions, the simulated MWDs (Figure 5D) were similar to that in Figure 3A. These simulations confirmed the subtle changes in the MWDs, especially for the higher molecular weights species, and provided further evidence for full conversion to the G3 dendrimer.

Parallel Synthesis of G3 Dendrimers Using a Variety of Polymeric Building Blocks. The parallel pathway was chosen in this section of work as it provided the most efficient and rapid route to the G3 dendrimer in one pot using Cu(I)Br/PMDETA in 50% DMSO/toluene for 30 min at 25 °C. We also wanted to show that our methodology could be used to create a wide range of G3 dendrimers with chemically different polymeric building blocks, including PSTY **10**, poly(*tert*-butyl acrylate) (P^tBA, **11**), poly(ethylene glycol) (PEG, **12**), and poly(*N*-isopropylacrylamide) (PNIPAM, **13**). These polymers were chosen

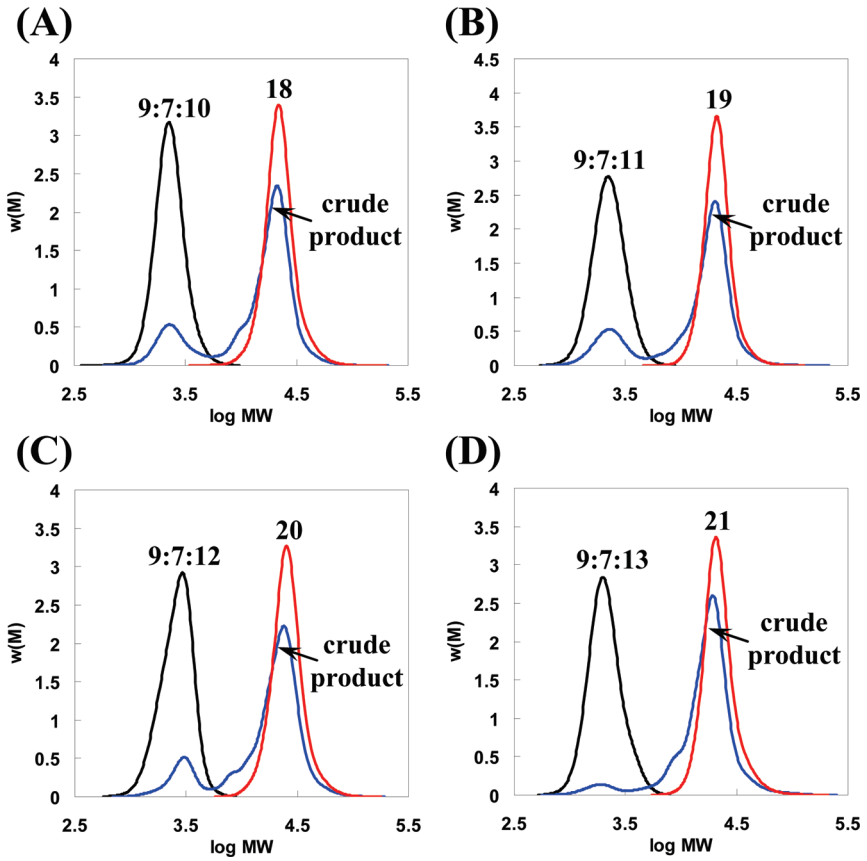

Figure 7. Size exclusion chromatography (SEC) traces for the synthesis of the G3 dendrimer via parallel technique with the P^{t}BA core (**9**) at 25 °C using DMSO as solvent and PMDETA as ligand. (A) P^{t}BA−PSTY$_4$−PSTY$_8$ (**18**); **9**:**7**:**10**:PMDETA:Cu(I)Br = 1:4.1:8.4:8:8, (B) P^{t}BA−PSTY$_4$−P^{t}BA$_8$ (**19**); **9**:**7**:**11**:PMDETA:Cu(I)Br = 1:4.1:8.4:8:8, (C) P^{t}BA−PSTY$_4$−PEG$_8$ (**20**); **9**:**7**:**12**:PMDETA:Cu(I)Br = 1:4.1:8.4:8:8, (D) P^{t}BA−PSTY$_4$−PNIPAM$_8$ (**21**); **9**:**7**:**13**:PMDETA:Cu(I)Br = 1:4.1:8.4:8:8.

for the following reasons: P^{t}BA can easily be converted to the hydrophilic poly(acrylic acid) which is a weak acid, PNIPAM becomes hydrophilic below its lower critical solution temperature (LCST) and aggregates above its LCST, and PEG (a hydrophilic polymer) has been widely used in biomedical applications. Typical syntheses of these polymers were given in the Experimental Section together with a comprehensive characterization of each polymer (Supporting Information). Absolute molecular weights were determined for all individual components (**7**−**12**) so that accurate stoichiometries could be used. The only exception was **13** as absolute SEC molecular weight determination was not possible. MALDI-ToF showed an $M_p \approx$ 2200, close to the M_n determined from SEC using PSTY standards, and $M_{n,NMR} \approx$ 2100 from ^{1}H NMR. For each G3 synthesis, a stoichiometry of 1:4.1:8.4 was used for the core, first generational layer, and second generational layer, respectively. The concentration of copper/ligand used was 8 times that of the starting core concentration, enough to fully catalyze both the NRC and CuAAC reactions.

The entire series of G3 polymeric dendrimer syntheses (Scheme 2) was based on two core polymers, PSTY and P^{t}BA, and four third generational layers consisting of PSTY, P^{t}BA, PNIPAM, and PEG. Each reaction was monitored by SEC (Figures 6 and 7) to ensure high yields of G3 dendrimers. Figure 6A shows the reaction of **7**, **8**, and **10** to produce **14** (G3[G1PSTY$_1$, G2PSTY$_4$, G3PSTY$_8$]) with high coupling efficiency (i.e., yield) after 30 min (Table 2). Because of the greater stoichiometries of the second and third generational layers starting polymer components, the final product contained a small amount of lower molecular weight reactants impurities and intermediate species from the coupling between reactants. The crude product was further purified by preparative SEC (red curve in Figure 6A). This provided an ideal method to purify complex polymer architectures. This should also be the method of choice when using these polymers in biomedical applications to obtain reproducible and consistent structures. The products for all other G3 dendrimers in Scheme 2 show that most of the reactants were converted to the G3 dendrimer with small amounts of lower molecular weight species and starting polymer (Figures 6 and 7). All G3 dendrimers after purification through the SEC preparative system gave near pure products (≥89%). The coupling efficiencies (see Table 2) for all G3 dendrimers were above 80%, with the only exception being product **20** (76%). The M_n and M_p values for all G3 dendrimers were all close to theory, and the polydispersity for all dendrimers was less than 1.14.

Further characterization by ^{1}H NMR showed the appearance of distinct peaks for each G3 polymeric dendrimer (see Supporting Information). The two aromatic protons, **b** and **c**, associated with the protons close to the TEMPO moiety appeared at chemical shifts of 7.6−7.8 and 8.0−8.2 ppm, respectively, and the peak associated with the CH_2 next to the azide from **7** shifted from 4.3 to 5.35 ppm, corresponding to the CH_2 (**d**) next to the triazole within the first generational layer. The proton corresponding

Scheme 4. Decoupling of G3 Polymeric Dendrimer (14) with 20 equiv of TEMPO-OH per Nitroxide in Toluene at 120 °C[a]

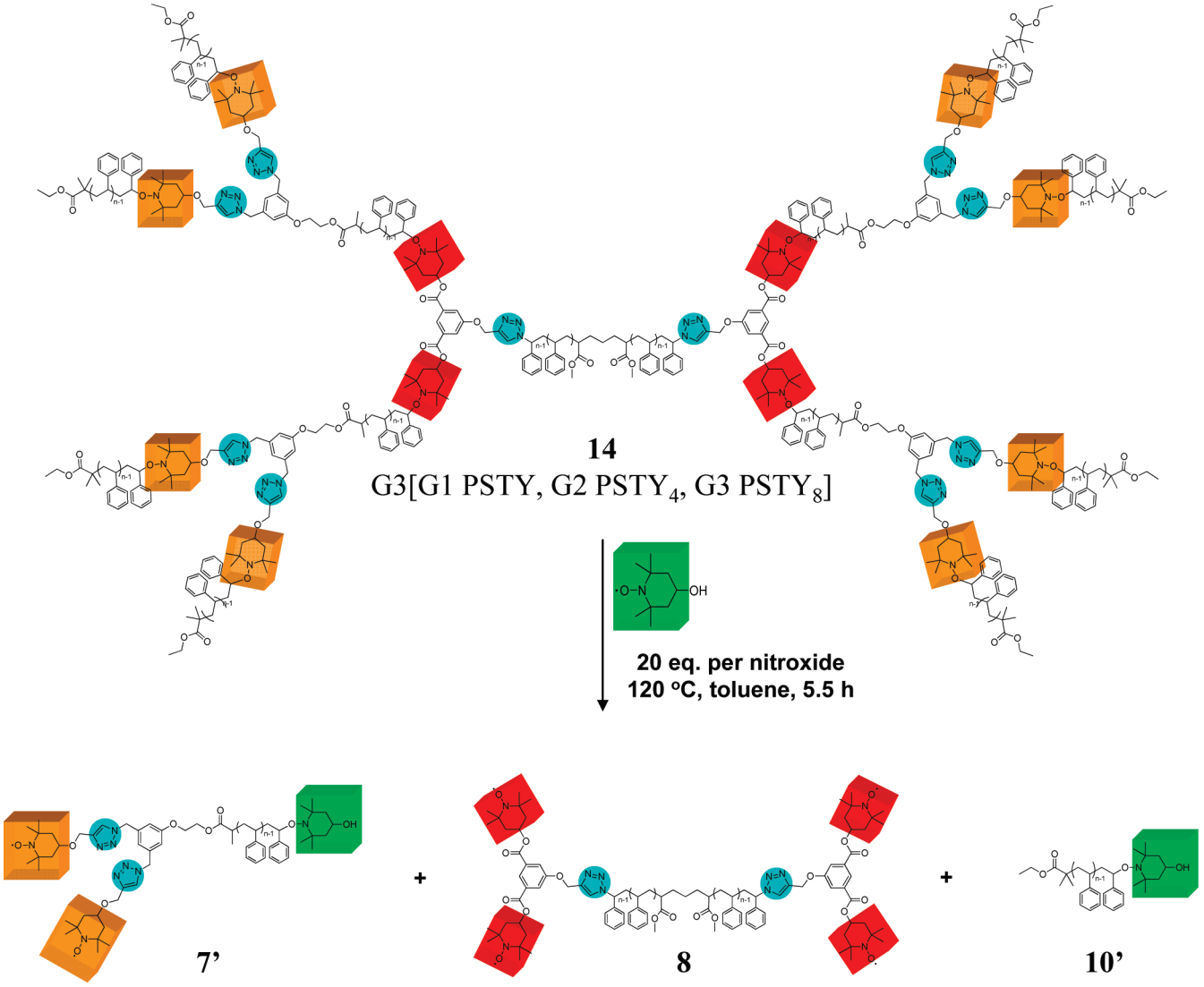

[a] Colored squares indicate TEMPO derivatives.

to the CH_2 (**e**) on the other side of the triazole appeared at various chemical shifts, depending on the polymer used as the peripheral layer. For PSTY, P^{t}BA, and PEG, this occurred between 4.60 and 4.65 ppm, and for PNIPAM, which has a slightly different substituent next to the functional alkyne (an ester group instead of an ether group), this occurred at 5.2 ppm. The proton associated with the CH on the triazole ring, **a**, appeared between 7.3 and 7.4 ppm, which can be obscured by the PSTY aromatic peaks. Along with these characteristic peaks, the peaks associated with the different side chains, backbone protons, and chain end protons of the various polymers also appeared and were labeled appropriately. All of these factors further support the formation of our desired polymer structures with minimal side reactions.

Decoupling of PSTY G3 Polymeric Dendrimer (14). Finally, to evaluate the efficiency of coupling to form the final polymeric dendrimer structure, a nitroxide exchange reaction (Scheme 4) was performed with TEMPO-OH at high temperature (120 °C) in a sealed flask with toluene.[21c−e] This type of reaction previously showed the reversibility at higher temperatures of alkoxyamines (formed through the NRC reactions) with 3-arm star, linear, and multiblock polymers.[21c,e] There was a 20 times excess of TEMPO-OH for each alkoxyamine, driving the reaction toward full exchange of nitroxide. The decoupling of **14** to its starting reagents showed that the degraded product had a similar MWD to the starting polymer blocks (Figure 8). The small difference was due to the difference in molecular weight between the original starting reagents and the products after degradation. Scheme 4 shows the entire range of products that would be generated from a nitroxide exchange reaction of **14** and TEMPO-OH. A small shoulder at higher molecular weight was also present, most likely due to incomplete exchange or side reactions from the exchange process. These impurities accounted for only 7% of the peak area based on a weight distribution, which would be considerably less based on a number distribution.

To further prove the reversibility of these G3 polymeric dendrimers, MALDI-ToF was used to analyze the final exchanged products (see products within Scheme 4). From the MALDI-ToF mass spectrum (Figure 9), two distributions can be observed. The first distribution ranging from 2500 to 3500 Da

dx.doi.org/10.1021/ma200649b |*Macromolecules* 2011, 44, 4814–4827

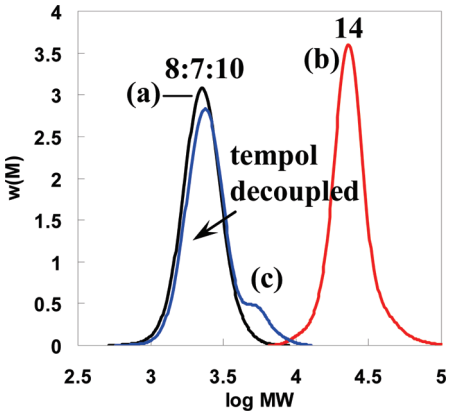

Figure 8. Size exclusion chromatography (SEC) MWD's for the synthesis of the PSTY G3 polymeric dendrimer (**14**) via a consecutive technique with the PSTY core (**8**) at 25 °C using DMSO as solvent and PMDETA as ligand and subsequent decoupling by TEMPO-OH exchange. Curves (a) starting reactants, (b) structure after purification through preparative SEC, and (c) decoupled dendrimer (20× excess TEMPO-OH per alkoxyamine, toluene, 120 °C, 5.5 h).

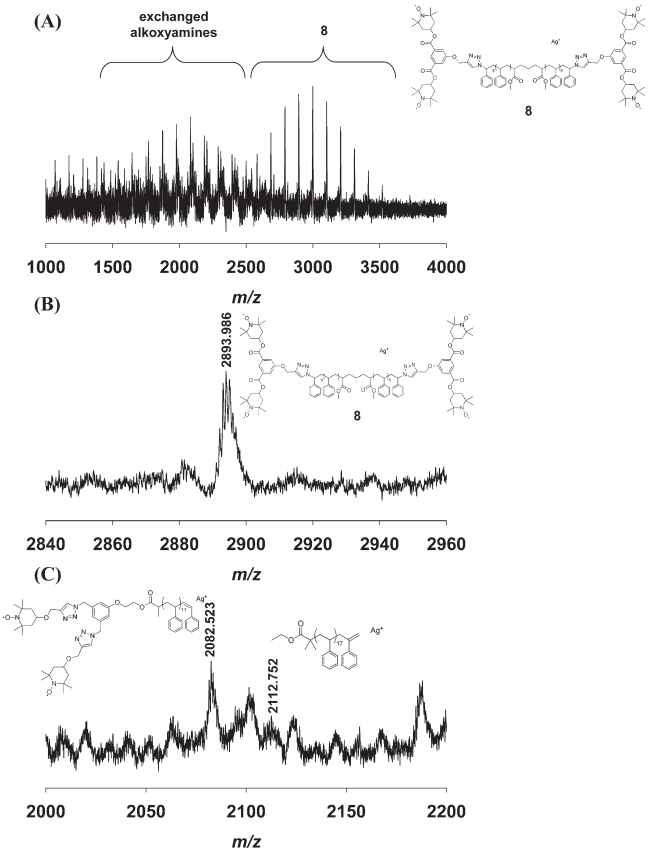

Figure 9. MALDI-ToF spectrum of G3 dendrimer, **14**, at 25 °C using DMSO as solvent and PMDETA as ligand; **8**:**7**:**10**:PMDETA:Cu(I)Br = 1:4.1:8.4:8:8, after decoupling with TEMPOL (20× excess TEMPO-OH per alkoxyamine, toluene, 120 °C, 5.5 h). (A) The entire distribution. (B) The expanded section of the higher MW distribution of the spectrum showing peaks with isotopic resolution. (C) The expanded section of the lower MW distribution of the spectrum showing peaks with isotopic resolution. The spectrum was recorded in linear mode using DCTB as the matrix and $AgCF_3COO$ was the cation source.

can be attributed to **8** (Figure 9B), and the second distribution (Figure 9C) ranging from 1000 to 2500 Da can be attributed to a combination of fragmentation products of **7′** and **10′** that are caused by MALDI-ToF chain-end degradation.[21c,32] Finally, we did not observe any high molecular weight species suggesting our G3 polymeric dendrimer (**14**) was of a high purity.

CONCLUSION

Through modulating the catalytic effect of the Cu(I) by changing ligand and solvent conditions, we could direct the rate of two orthogonal "click"-type reactions: CuAAC and NRC. Using the model PSTY building block system, third generation dendrimers could be formed divergently, convergently, or in parallel through modulating the Cu(I) activity. The combination of Me_6TREN ligand with 30% DMSO and 70% toluene resulted in a divergent pathway, in which the formation of the second generation dendrimer by SET-NRC was completed in less than 2 min, followed by the coupling of the third generational layer in 30 min. Changing the ligand to PMDETA and using 50% DMSO and 50% toluene gave similar rates of CuAAC and NRC, resulting in the G3 dendrimer formation through a parallel process. Using PMDETA and 100% toluene gave a much faster CuAAC reaction than NRC. The dendron was formed first after a few minutes, but the coupling of the dendrons to the core was slow, taking up to 24 h—a convergent pathway. To increase the speed of the convergent pathway, 15% DMSO was added as a cosolvent. The reaction was now complete in under 2 h. Simulations of the MWDs showed the generation of the intermediated species and confirmed the formation of G3 dendrimers. This G3 dendrimer can be cleaved at the alkoxyamine sites to linear polymers through heating at 120 °C in the presence of an excess hydroxy nitroxide. The results given in this work show the orthogonal nature of both the NRC and CuAAC reactions and their dependence on the Cu(I) activity.

The utility of this new approach allowed us to produce third generational layered dendrimers in one pot at 25 °C in under 30 min using solvent and ligand conditions to facilitate the parallel process. The range of dendrimers formed were in high yields through coupling linear telechelic polymer building blocks, consisting of PSTY, P^{t}BA, PEG, and PNIPAM. Preparative SEC was used to fractionate starting reactants and intermediate polymer species.

ASSOCIATED CONTENT

Supporting Information. Synthesis and characterizations of all the TEMPO derivatives, experimental details of end-group modification reactions, all the ^{1}H NMR spectra, MALDI-ToF, MS SEC traces, ESI-MS spectra, and UV−vis spectra. This material is available free of charge via the Internet at http://pubs.acs.org.

AUTHOR INFORMATION

Corresponding Author

*E-mail: m.monteiro@uq.edu.au.

ACKNOWLEDGMENT

M.J.M. acknowledges financial support from the ARC Discovery grant (DP0987315), and Z.J. acknowledges the UQ Postdoctoral Research Fellowship.

REFERENCES

(1) (a) Boyer, C.; Stenzel, M. H.; Davis, T. P. *J. Polym. Sci., Part A: Polym. Chem.* **2011**, *49*, 551–595. (b) Hadjichristidis, N.; Pitsikalis, M.; Iatrou, H.; Sakellariou, G. *Controlled Living Polym.* **2009**, 343–443. (c) Matyjaszewski, K.; Tsarevsky, N. V. *Nature Chem.* **2009**, *1*, 276–288. (d) Qin, A.; Lam, J. W. Y.; Tang, B. Z. *Macromolecules* **2010**, *43*, 8693–8702. (e) Sumerlin, B. S.; Vogt, A. P. *Macromolecules* **2010**, *43*, 1–13.

(2) (a) Kolb, H. C.; Finn, M. G.; Sharpless, K. B. *Angew. Chem., Int. Ed.* **2001**, *40*, 2004–2021. (b) Lutz, J.-F. *Angew. Chem., Int. Ed.* **2007**, *46*, 1018–1025.

(3) (a) Okcu, S. S.; Durmaz, Y. Y.; Yagci, Y. *Des. Monomers Polym.* **2010**, *13*, 459–472. (b) Zhang, W.; Mueller, A. H. E. *Macromolecules* **2010**, *43*, 3148–3152. (c) Degirmenci, M.; Genli, N. *Macromol. Chem. Phys.* **2009**, *210*, 1617–1623.

(4) (a) Topham, P. D.; Sandon, N.; Read, E. S.; Madsen, J.; Ryan, A. J.; Armes, S. P. *Macromolecules* **2008**, *41*, 9542–9547. (b) Vogt, A. P.; Sumerlin, B. S. *Macromolecules* **2006**, *39*, 5286–5292.

(5) Hu, D.; Zheng, S. *Eur. Polym. J.* **2009**, *45*, 3326–3338.

(6) (a) Laurent, B. A.; Grayson, S. M. *J. Am. Chem. Soc.* **2006**, *128*, 4238–4239. (b) Lonsdale, D. E.; Bell, C. A.; Monteiro, M. J. *Macromolecules* **2010**, *43*, 3331–3339. (c) Lonsdale, D. E.; Monteiro, M. J. *Chem. Commun.* **2010**, *46*, 7945–7947. (d) Dong, Y.-Q.; Tong, Y.-Y.; Dong, B.-T.; Du, F.-S.; Li, Z.-C. *Macromolecules* **2009**, *42*, 2940–2948. (e) Eugene, D. M.; Grayson, S. M. *Macromolecules* **2008**, *41*, 5082–5084.

(7) (a) Whittaker, M. R.; Urbani, C. N.; Monteiro, M. J. *J. Am. Chem. Soc.* **2006**, *128*, 11360–11361. (b) Lammens, M.; Fournier, D.; Fijten, M. W. M.; Hoogenboom, R.; Du Prez, F. *Macromol. Rapid Commun.* **2009**, *30*, 2049–2055.

(8) (a) Urbani, C. N.; Bell, C. A.; Lonsdale, D.; Whittaker, M. R.; Monteiro, M. J. *Macromolecules* **2008**, *41*, 76–86. (b) Urbani, C. N.; Bell, C. A.; Whittaker, M. R.; Monteiro, M. J. *Macromolecules* **2008**, *41*, 1057–1060. (c) Urbani, C. N.; Lonsdale, D. E.; Bell, C. A.; Whittaker, M. R.; Monteiro, M. J. *J. Polym. Sci., Part A: Polym. Chem.* **2008**, *46*, 1533–1547.

(9) (a) Pan, P.; Fujita, M.; Ooi, W.-Y.; Sudesh, K.; Takarada, T.; Goto, A.; Maeda, M. *Polymer* **2011**, *52*, 895–900. (b) Lutz, J.-F.; Boerner, H. G.; Weichenhan, K. *Macromolecules* **2006**, *39*, 6376–6383.

(10) (a) Xu, L. Q.; Wan, D.; Gong, H. F.; Neoh, K.-G.; Kang, E.-T.; Fu, G. D. *Langmuir* **2010**, *26*, 15376–15382. (b) Chen, J.; Xiang, J.; Cai, Z.; Yong, H.; Wang, H.; Zhang, L.; Luo, W.; Min, H. *J. Macromol. Sci., Part A: Pure Appl. Chem.* **2010**, *47*, 655–662. (c) Chen, J. C.; Luo, W. Q.; Wang, H. D.; Xiang, J. M.; Jin, H. F.; Chen, F.; Cai, Z. W. *Appl. Surf. Sci.* **2010**, *256*, 2490–2495.

(11) Sumerlin, B. S.; Vogt, A. P. *Macromolecules* **2010**, *43*, 1–13.

(12) Inglis, A. J.; Sinnwell, S.; Stenzel, M. H.; Barner-Kowollik, C. *Angew. Chem., Int. Ed.* **2009**, *48*, 2411–2414.

(13) (a) Killops Kato, L.; Campos, L. M.; Hawker, C. J. *J. Am. Chem. Soc.* **2008**, *130*, 5062–5064. (b) Montanez, M. I.; Campos, L. M.; Antoni, P.; Hed, Y.; Walter, M. V.; Krull, B. T.; Khan, A.; Hult, A.; Hawker, C. J.; Malkoch, M. *Macromolecules* **2010**, *43*, 6004–6013. (c) Antoni, P.; Robb, M. J.; Campos, L. M.; Montanez, M. I.; Hult, A.; Malmstrom, E.; Malkoch, M.; Hawker, C. J. *Macromolecules* **2010**, *43*, 6625–6631.

(14) Grayson, S. M.; Frechet, J. M. J. *Chem. Rev.* **2001**, *101*, 3819–3867.

(15) (a) Tekade, R. K.; Kumar, P. V.; Jain, N. K. *Chem. Rev.* **2009**, *109*, 49–87. (b) Lee, C. C.; MacKay, J. A.; Frechet, J. M. J.; Szoka, F. C. *Nature Biotechnol.* **2005**, *23*, 1517–1526.

(16) (a) Newkome, G. R.; Yao, Z.; Baker, G. R.; Gupta, V. K. *J. Org. Chem.* **1985**, *50*, 2003–2004. (b) Tomalia, D. A.; Baker, H.; Dewald, J.; Hall, M.; Kallos, G.; Martin, S.; Roeck, J.; Ryder, J.; Smith, P. *Polym. J.* **1985**, *17*, 117–132.

(17) (a) Ihre, H.; Hult, A.; Frechet, J. M. J.; Gitsov, I. *Macromolecules* **1998**, *31*, 4061–4068. (b) Hawker, C. J.; Frechet, J. M. J. *J. Am. Chem. Soc.* **1990**, *112*, 7638–7647. (c) Onitsuka, K.; Fujimoto, M.; Ohshiro, N.; Takahashi, S. *Angew. Chem., Int. Ed.* **1999**, *38*, 689–692. (d) Ashton, P. R.; Boyd, S. E.; Brown, C. L.; Jayaraman, N.; Stoddart, J. F. *Angew. Chem., Int. Ed.* **1997**, *36*, 732–735.

(18) (a) Antoni, P.; Hed, Y.; Nordberg, A.; Nystrom, D.; von Holst, H.; Hult, A.; Malkoch, M. *Angew. Chem., Int. Ed.* **2009**, *48*, 2126–2130. (b) Wu, P.; Feldman, A. K.; Nugent, A. K.; Hawker, C. J.; Scheel, A.; Voit, B.; Pyun, J.; Frechet, J. M. J.; Sharpless, K. B.; Fokin, V. V. *Angew. Chem., Int. Ed.* **2004**, *43*, 3928–3932.

(19) Ma, X.; Tang, J.; Shen, Y.; Fan, M.; Tang, H.; Radosz, M. *J. Am. Chem. Soc.* **2009**, *131*, 14795–14803.

(20) (a) Matyjaszewski, K. *Curr. Org. Chem.* **2002**, *6*, 67–82. (b) Matyjaszewski, K.; Woodworth, B. E.; Zhang, X.; Gaynor, S. G.; Metzner, Z. *Macromolecules* **1998**, *31*, 5955–5957. (c) Pintauer, T.; Matyjaszewski, K. *Chem. Soc. Rev.* **2008**, *37*, 1087–1097. (d) Fu, Q.; Lin, W. C.; Huang, J. L. *Macromolecules* **2008**, *41*, 2381–2387. (e) Fu, Q.; Wang, G. W.; Lin, W. C.; Huang, J. L. *J. Polym. Sci., Part A: Polym. Chem.* **2009**, *47*, 986–990. (f) Luo, X. L.; Wang, G. W.; Huang, J. L. *J. Polym. Sci., Part A: Polym. Chem.* **2009**, *47*, 59–68.

(21) (a) Jia, Z.; Bell, C. A.; Monteiro, M. J. *Chem. Commun.* **2011**, *47*, 4165–4167. (b) Jia, Z.; Bell, C. A.; Monteiro, M. J. *Macromolecules* **2011**, *44*, 1747–1751. (c) Kulis, J.; Bell, C. A.; Micallef, A. S.; Jia, Z.; Monteiro, M. J. *Macromolecules* **2009**, *42*, 8218–8227. (d) Kulis, J.; Bell, C. A.; Micallef, A. S.; Monteiro, M. J. *J. Polym. Sci., Part A: Polym. Chem.* **2010**, *48*, 2214–2223. (e) Kulis, J.; Bell, C. A.; Micallef, A. S.; Monteiro, M. J. *Aust. J. Chem.* **2010**, *63*, 1227–1236.

(22) (a) Percec, V.; Guliashvili, T.; Ladislaw, J. S.; Wistrand, A.; Stjerndahl, A.; Sienkowska, M. J.; Monteiro, M. J.; Sahoo, S. *J. Am. Chem. Soc.* **2006**, *128*, 14156–14165. (b) Percec, V.; Popov, A. V.; Ramirez-Castillo, E.; Monteiro, M.; Barboiu, B.; Weichold, O.; Asandei, A. D.; Mitchell, C. M. *J. Am. Chem. Soc.* **2002**, *124*, 4940–4941.

(23) Wang, J.-S.; Matyjaszewski, K. *Macromolecules* **1995**, *28*, 7901–7910.

(24) Geng, J.; Lindqvist, J.; Mantovani, G.; Haddleton, D. M. *Angew. Chem., Int. Ed.* **2008**, *47*, 4180–4183.

(25) Ciampolini, M.; Nardi, N. *Inorg. Chem.* **1966**, *5*, 41–44.

(26) Urbani, C. N.; Monteiro, M. J. *Macromolecules* **2009**, *42*, 3884–3886.

(27) (a) Rosen, B. M.; Jiang, X.; Wilson, C. J.; Nguyen, N. H.; Monteiro, M. J.; Percec, V. *J. Polym. Sci., Part A: Polym. Chem.* **2009**, *47*, 5606–5628. (b) Rosen, B. M.; Percec, V. *Chem. Rev.* **2009**, *109*, 5069–5119.

(28) Pintauer, T.; Reinol, U.; Feth, M.; Bertagnolli, H.; Matyjaszewski, K. *Eur. J. Inorg. Chem.* **2003**, 2082–2094.

(29) Pintauer, T.; Matyjaszewski, K. *Coord. Chem. Rev.* **2005**, *249*, 1155–1184.

(30) Frechet, J. M. J., Tomalia, D., Eds.; Wiley and Sons: New York, 2001.

(31) Cabaniss, S. E.; Zhou, Q.; Maurice, P. A.; Chin, Y.-P.; Aiken, G. R. *Environ. Sci. Technol.* **2000**, *34*, 1103–1109.

(32) Ladaviere, C.; Lacroix-Desmazes, P.; Delolme, F. *Macromolecules* **2009**, *42*, 70–84.